Using structural MRI and DTI to map plastic changes in the mouse brain resulting from deep brain stimulation

M. M. Chakravarty[1,2], C. Hamani[3,4], J. Ellegood[1], M. Diwan[3], C. Laliberté[1], J. Bishop[1], J. Dazai[1], B. J. Nieman[1], J. N. Nobrega[3], R. M. Henkelman[1], and J. P. Lerch[1]

[1]Mouse Imaging Centre (MICe), The Hospital for Sick Children, Toronto, Ontario, Canada, [2]Rotman Research Institute, Baycrest, Toronto, Ontario, Canada, [3]Neuroimaging Research Section, Centre for Addiction and Mental Health, Toronto, Ontario, Canada, [4]Division of Neurosurgery, Toronto Western Hospital, Toronto, Ontario, Canada

Introduction: Deep brain stimulation (DBS), a surgical procedure in which a stimulating electrode is implanted in the brain, has been used successfully to alleviate symptoms in pharmacologically intractable cases of Parkinson's disease and other movement disorders. Novel surgical targets for DBS are currently being investigated in the context different neurological dysfunctions. In this study, we specifically investigate the impact of this procedure on a target used in treatment resistant depression; namely the subcallosal cingulate [1]. Despite the initial reports of the clinical efficacy of this procedure, the mechanisms of action and the sensitivity of the brain to stimulation parameters are poorly understood [1,2]. While some work has been done on characterizing the pre- and post-operative behaviour rats [2,3], little has been done to determine if plasticity of the brain in response to DBS is part of the mechanism of action. In this study, we use high-resolution anatomical and diffusion tensor magnetic resonance imaging (MRI) data to examine the plasticity of mouse neuroanatomy in response to DBS of the anterior cingulate in the mouse.

Materials and Methods: Twenty-four nine-week-old C57BL/6 were examined in this study: 8 controls (CTL), 8 with deep brain stimulator implanted (SHAM), and 8 who received DBS. A week after implantation, the DBS group received stimulation for six hours a day over five days (stimulation parameters: 200 µA, 130 Hz, 90µsec pulse width). Mice were perfused through the left ventricle with 30 mL of phosphate-buffered saline (PBS) (pH 7.4) at room temperature (25 °C). This was followed by infusion with 30 mL of 4% paraformaldehyde (PFA) and 2mM of ProHance® (Bracco Diagnostics Inc., Princeton, NJ) in PBS at room temperature. Following perfusion, the heads were removed along with the skin, lower jaw, ears and the cartilaginous nose tip. The remaining skull structures containing the brain were allowed to postfix in 4% PFA and 2mM of ProHance® at 4 °C for 12 h. A multi-channel 7.0 T MRI scanner (Varian Inc., Palo Alto, CA) was used to acquire anatomical images of brains within skulls [4]. Prior to imaging, the samples were removed from the contrast agent solution, blotted and placed into 13-mm-diameter plastic tubes filled with a proton-free susceptibility-matching fluid (Fluorinert FC-77, 3M Corp., St. Paul, MN). An array of 16 custom built solenoid coils was used for high-throughput scanning of the specimens using a T2-weighted fast spin echo sequence, TR/TE=2000/42 ms, 2 averages, field-of-view=2.5x1.4x1.4 cm^3, image matrix size=250x252x450, giving an image with 56 µm voxels (total imaging time ~13 hours). Using a 6cm inner bore diameter insert gradient, additional 3D diffusion weighted fast spin-echo sequences were acquired using the standard method [5] (imaging parameters: echo train length of 6 was used with a TR=325 ms, first TE=30 ms, and a TE=6 ms echo spacing for the remaining 5 echoes, two averages, field-of-view= 1.4x1.4x2.5cm^3 and a matrix size of 108x108x192, 130 µm isotropic voxels; diffusion parameters: ∂= 4ms, Δ= 15ms, five b=0 s/mm^2 images, and 30 high b-value images, b=1917 s/mm^2 in 30 different directions). Three custom-built, solenoid coils with over wound ends were used to image three brains in parallel [6]. Total imaging time was ~12 hours.

Anatomical changes caused by DBS were estimated using deformation-based analysis of the T2-weighted MRI data (as described in previous publications from our group [7]). All MRI volumes were rigidly rotated and translated (3 rotations and 3 translations) to match an initial atlas. All possible pair-wise 12-parameter transformations (3 rotations, translations, scales and shears) [8] were estimated and an average linear transformation was calculated for each image, thus effectively scaling each brain to the average size of the population. After applying the average transformation, MRI volumes were averaged in order to create a first population-based model. A multi-generation, multi-resolution fitting strategy was then initialized where each brain is nonlinearly registered [9] to the 12-parameter population atlas, and subsequently to the atlas of the previous nonlinear registration. The final deformation fields map each T2-weighted volume to the average of the entire population. The Jacobian determinant [10], a measure of local expansion and contraction, was estimated at each node in the final deformation fields. Fractional anisotropy (FA) and mean diffusivity (MD) were estimated using the FSL software package [11]. The B0 images were used to create a separate group model using the method described above. Final transformations were applied to FA and MD maps to align them in a common space. Voxel-wise analysis was conducted using the RMINC software package.

Results: Voxel-based analysis of the deformation fields show significant local volumetric increases (after correcting for false discovery rate [12] of <5%) of the DBS group in comparison to the CTL in the left hippocampus (See Fig 1). No significant differences were observed between the SHAM and DBS groups. As expected, volume increases were also found at the site of the DBS implantation. In the analysis of the DTI data, no differences in the voxel-wise FA values were found. However, mean diffusivity is significantly decreased in the region of the amygdala of the DBS animals in comparison to the CTL (see Fig 2). Although no significant differences were found between SHAM/CTL and DBS/SHAM comparisons, there are trends suggesting an increase on hippocampal volume and decrease of MD in the SHAM group.

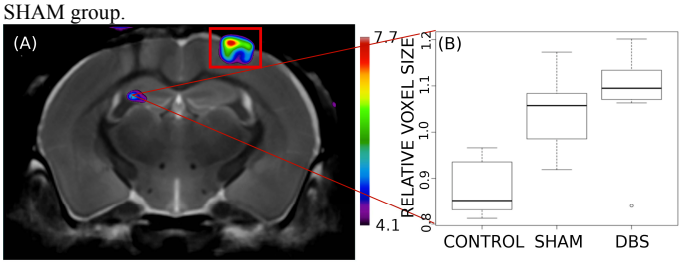

Figure 1. Local volumetric changes of the left hippocampus. (A) Voxel-wise statistics. Region in boxed area indicates volumetric changes due to insertion of ground screws. (B) Local expansions at peak location in the hippocampus. Colour bar represents t-statistic values.

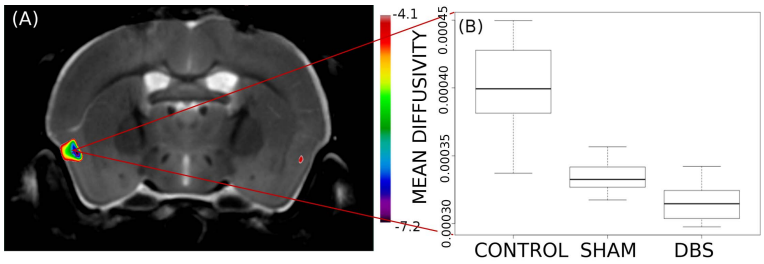

Figure 2. Local changes in MD of the left amygdala. (A) Voxel-wise decreases in MD in amygdala. (B) MD values at minimum voxel location. Colour bar represents t-statistic values.

Conclusions: This is the first example of automated MRI-based anatomical analysis in surgical mouse models. The methodology used is capable of simultaneously accommodating lesions introduced by the DBS electrode and elucidating anatomical changes distal to the lesion site. The results demonstrate the plasticity of the brain in response to DBS of the ventromedial prefrontal cortex. Further, the results demonstrate the lesioning by itself may play a role in neuronal remodeling; however DBS may be accelerating or maintaining plastic changes in comparison to sham lesions. In particular, local changes are observed in anatomical regions implicated in depression; specifically the volumetric expansion of the hippocampus and the decrease of MD in the amygdala may provide insight with respect to the neuronal remodeling taking place after successful DBS of the anterior cingulate in patients suffering from treatment resistant depression.

References: [1] Lozano *et al.* Biological Psychiatry 64(6):461-7. [2] Hamani *et al.* Biological Psychiatry 67(2):117-24. [3] Hamani *et al.* Journal of Psychiatric Research 44(11):683-7. [4] Nieman *et al.* NMR in Biomedicine. [5] Jones *et al.* Magnetic Resonance in Medicine 42(3):515-25. [6]Ellegood *et al.* NeuroImage 53(3): 1023-9. [7] Lerch *et al.* NeuroImage 39(1):32-9. [8] Collins *et al.* Journal of Computer Assisted Tomography 18(2):192-205. [9] Collins *et al*. Human Brain Mapping 3(3):190-208. [10] Chung *et al.* NeuroImage 14(3):595-606. [11] Smith *et al.* NeuroImage 23(S1):S208-19. [12] Genovese *et al.* NeuroImage 15(4):870-8.